Efficient recovery of nitrate from municipal wastewater via MCDI using anion-exchange polymer coated electrode embedded with nitrate selective resin

David Inhyuk Kim[ab], Ralph Rolly Gonzales[a], Pema Dorji[a], Gimun Gwak[a], Sherub Phuntsho[a], Seungkwan Hong[b], HokyongShon[a]

[a]Centre for Technology in Water and Wastewater, School of Civil and Environmental Engineering, University of Technology, Sydney (UTS), 15 Broadway, NSW 2007, Australia

[b]School of Civil, Environmental & Architectural Engineering, Korea University, 145, Anam-ro, Seongbuk-gu, Seoul 02841, Republic of Korea

Abstract

A NO_3^-—selective carbon electrode coated with an anion-selective polymer with polystyrenic macroporous nitrate—selective A520E resin particles (in chloride form; particle size: 300–1200 μm) was fabricated for desalination of municipal wastewater and NO_3^- recovery during membrane capacitive deionization (MCI). Several issues, such as electrosorption/regeneration efficiency, selectivity of NO_3^-, and removal from real wastewater, were addressed to demonstrate the suitability of coated electrodes. The NO_3^-—selective electrode induced better electrosorption than the conventional MCDI, whereas its salt adsorption capacity was lower than that of the ion-exchange (IX) layer only coated one. The mole fraction of NO_3^- adsorption kept increased even after saturation by replacing Cl^- adsorbed on the resin coating layer. However, the desorption efficiency of NO_3^- was retarded as it was exchanged with Cl^- and temporarily intercepted in the resin of the IX layer, during ion migration towards the bulk brine solution. 81.5% of NO_3^- was removed with better NO_3^- selectivity from real municipal wastewater, and a high concentration of NO_3^- brine was obtained through successive operation. However, the poorly selective NO_3^- desorption, which limits its enrichment due to the reverse ionic-strength gradient induced by the high concentration brine, needs to be mitigated to prove its effective recovery.

Introduction

There is a currently increasing demand for clean water brought about by the continuous growth of the world's population and economy, as well as industrialization (Shannon, Bohn et al. 2008, Chung, Li et al. 2012, Park, Lim et al. 2019). Among the solutions in augmenting, the clean water supply are desalination and wastewater reuse. Wastewater reuse does not only mitigate water scarcity, but also address problems with environmental pollution and resource recovery (Ansari, Hai et al. 2017). In fact, resource recovery is highly important in meeting the strict effluent discharge standards prior to disposal of wastewater (Batstone, Hülsen et al. 2015).

Among these substances present in wastewater is nitrate (NO_3^-), one of the inorganic forms of nitrogen, which is formed from the oxidation of ammonia. This ion is mostly considered as a pollutant whose effect, when consumed, can cause health problems such as reduced fertility, increased levels of methemoglobin in infants, stillbirths, and even death (Kim and Choi 2012). Removal of NO_3^- has been performed in literature through a number of various methods: biological treatment (Watsuntorn, Ruangchainikom et al. 2019), ion exchange (IX) (Bae, Jung et al. 2002), electrocoagulation (Karamati-Niaragh, Alavi Moghaddam et al. 2019), catalysis (Mendow, Veizaga et al. 2019), ultrafiltration (Bahmani, Maleki et al. 2019, Gao, Wang et al. 2019), reverse osmosis (Schoeman and Steyn 2003, Epsztein, Nir et al. 2015), electrodialysis (Menkouchi Sahli, Annouar et al. 2008), and adsorption (Senthil Kumar, Yaashikaa et al. 2019). While these processes can remove or recover NO_3^-, each process has its own limitations and challenges. Biological treatment requires microorganisms that are highly sensitive to various stimuli and

conditions, as well as large bioreactors that offset its relatively low cost (Park and Yoo 2009). IX may be able to efficiently remove NO_3^-; however, this process results to a huge amount of waste generated from the IX resin required (Bae, Jung et al. 2002).

Capacitive deionization (CDI), the adsorption of ions of opposite charges onto a porous carbon electrode after the application of electric potential, is an emerging process for desalination of low salinity water and resource recovery (Oren 2008, Porada, Zhao et al. 2013). Among the reasons, this process has attracted research attention for its ability to remove ions from a feed solution by means of electrosorption without the extensive use of energy and the generation of brine waste during operation. Not only CDI is an efficient process in desalting and resource recovery, it is also environmentally friendly. CDI has particularly gained a niche application with the treatment of low salinity water, such as brackish water (which contains 2000 to 10000 ppm of solutes) (Koparal and Öğütveren 2002). Treatment of such wastewater solutions is considered non-economical using conventional membrane processes, due to the energy expenditure associated with these processes.

A particular topic of interest in the study of CDI is the development of various carbon-based electrodes to improve the adsorption capacity of the electrodes and the charge efficiency (Li, Zou et al. 2010, Jia and Zou 2012, Nie, Pan et al. 2012). This particular interest has led to the development of the membrane capacitive deionization (MCDI), a process involving a pair of carbon electrodes coupled with ion exchange membranes (IEMs) (Biesheuvel and van der Wal 2010, Kim and Choi 2010). MCDI has shown to improve the electrosorption and regeneration efficiencies significantly due to the presence of the IEMs, which adsorb either cations or anions, regardless of the ion type, charge, and size. While the presence of IEMs has significantly enhanced the performance of MCDI,

a better application of MCDI electrode development is custumization of the electrodes targeted for specific ion/s that can be used for treatment of a multi-component solution.

Selective removal of NO_3^- using MCDI has been done a few times in previous studies. Batch mode CDI was attempted by Tang et al, wherein they used CDI to remove NO_3^- and F^- present in a synthetic brackish groundwater solution (Tang, Kovalsky et al. 2015). To demonstrate that MCDI operation can be varied to selectively remove NO_3^-, the applied current during MCDI operation was varied in another study (Kim, Kim et al. 2013). The researchers found out that the mole fraction of NO_3^- relative to all the other ions adsorbed by the MCDI electrode were inversely proportional to the applied current, i.e. less applied current showed lower NO_3^- adsorption.

Development of NO_3—selective electrode for MCDI has also been a topic of interest in recent. Yeo and Choi in 2013 (Yeo and Choi 2013) fabricated a NO_3—selective carbon electrode using an anion exchange resin with high NO_3^- selectivity. While the amount of adsorbed ions were similar compared to a nascent electrode, the amount of NO_3^- ions adsorbed on the developed electrode was twice higher. Kim and Choi (Kim and Choi 2012) developed the first reported nitrate-selective composite carbon electrodes for CDI. In their study, the carbon electrode surface was coated with highly NO_3—selective BHP55 anion exchange resin. The resultant electrode's NO_3^- removal was compared with that of the conventional MCDI electrode, and it was found that the NO_3^- adsorption was 2.3 times higher than the conventional MCDI electrode. Despite the improvement of NO_3^- removal performance, selectivity could have been further improved with the use of another resin. Another recent NO_3—specific MCDI study was conducted by Gan et al (Gan, Wu et al. 2019), wherein they developed a double-layer composite electrodes after coating activated carbon electrodes with A520E anion exchange resin on one side and

carboxyl-functionalized multi-walled carbon nanotubes on the other. The asymmetric nature of the electrode showed enhanced NO_3^- selectivity, despite the use of other binary anion solutions, such as those containing SO_4^{2-}, F^-, and Cl^-. Another issue in these studies is that the improved selectivity for NO_3^- was demonstrated using synthetic solutions of high NO_3^- concentrations, when in fact NO_3^- only exists in low concentrations compared to other anions in wastewater. Another problem in the development of electrodes for MCDI is the use of organic polymers, such as PVDF, as binders. These polymers are known to have high electrical resistance, which then hampers the deionization process (Yeo and Choi 2013).

In this study, a NO_3—selective activated carbon electrode with enhanced selective adsorption of NO_3^- in a multi-component solution was developed for effective NO_3^- recovery during an MCDI wastewater reclamation process. The activated carbon electrode was coated with an IX polymer solution containing A520E NO_3—selective resin. The electrosorption performance of the coated electrode was first tested at a lab-scale MCDI unit. Its performance was also compared with an electrode coated by the IX solution only. The selectivity of NO_3^- from a mixture of selected anions during electrosorption and electrode regeneration was then investigated. Lastly, the applicability of the used electrodes was discussed based on the results of the five successive cycle operation of MCDI using real municipal wastewater.

Materials and methods

Fabrication of the ion-exchange polymer coated carbon electrode with embedded A520E

The carbon electrodes provided by Siontech Co. (Republic of Korea) were composed of a graphite body sheet coated with a carbon slurry blended with activated carbon, P-60 (Kuraray Chemical Co., Japan) and polyvinylidene fluoride (Inner Mongolia 3F-Wanhao Fluorine Chemical Co., China).

The cathode used for the experiments was coated with a cation-exchange polymer solution containing sulfonic acid group. The IX capacity of the dry cation-exchange polymer was reported to be 1.7 meq/g in average. A 20 wt % solution of the cation—selective polymer with N-methyl-2-pyrrolidone (NMP, Sigma-Aldrich, USA) was vigorously stirred at 20 ºC for 24 hr.

Then, two electrodes coated with different anion-exchange layers were used as anodes to compare their performance. An anion-exchange polymer was prepared by introducing tertiary amine groups after the chloromethylation of polystyrene (Kim and Choi 2012). The IX capacity of the dry anion-exchange polymer was reported to be 1.5 meq/g in average. The anion-exchange polymer was mixed with NMP and stirred at 20 ºC for 24 hr to produce a 17 wt % solution. The control anode (IX layered electrode) was activated carbon electrode coated with this anion-exchange polymer solution. Prior to the preparation of the other anode, NO_3—selective A520E resin was dried at 80ºC for 24 hr, pulverized with a ball mill and was then sieved with a 50 um stainless-steel mesh, and mixed with the 12 wt % anion-exchange polymer solution with a polymer-to-resin weight ratio of 1:1. Another activated carbon electrode was coated with the anion-exchange polymer solution containing A520E NO_3—selective resin to produce A520E/IX layered electrode. The anion-selective electrodes were coated with the uniformly mixed coating solutions using a casting machine (Elcometer 4340, Elcometer (Asia) Pte Ltd, Singapore), and dried at 50ºC for 12 hr. The dried samples were then stored in DI water at 4 ºC.

Surface morphology of the coated electrodes was characterized using a field emission scanning electron microscopy (FE-SEM) (Zeiss Supra 55VP, Carl Zeiss AG, Germany) (Park, Gonzales et al. 2018).

Bench-scale MCDI using ion-exchange layer-coated electrodes

The MCDI experiments were carried out using a lab-scale flow-through system as described in our previous work (Kim, Gwak et al. 2017). The dimensions of the rectangular flow channel of the test cell were 10x10 cm with an effective adsorption area of 100 cm^2. A pair of cation- and anion-exchange electrodes was symmetrically placed within the test cell, separated by a non-conductive nylon spacer between these two electrodes ensuring flow of water and preventing short-circuiting (Dorji, Choi et al. 2018). The influent water was brought entirely into contact with the IX layer-coated electrodes by punching a 1 cm diameter sized hole in the center of the electrodes and mesh spacer. A peristaltic pump (Cole-Palmer, USA) was used to circulate the influent throughout the MCDI unit with a constant flow rate of 30 mL/min. A constant level of electrical potential was applied through the MCDI unit by a potentiostat, WPG-100 (WonATech Co., Republic of Korea). The system was stabilized prior to the test runs by flushing out the feed solution through the system under single-pass mode at 0 V, until the readings of conductivity and pH were to be the same to those of in feed. All the tests were duplicated at 20 ^oC.

.

Investigation of preferential electrosorption and discharge of nitrate using A520E/IX electrode

A synthetic mixed solution containing 3.3 mM each of NaCl, Na_2SO_4, and $NaNO_3$ was flowed into the lab-scale system for 450 s at a 1.2 V applied potential under single-pass mode. The electrodes were then regenerated by short-circuiting under single-pass mode. During the regeneration, DI water was fed through the system at -1.2 V for 450 s, and the effluent was collected each 30 s. After each run, complete regeneration of the carbon electrodes was ensured by employing an additional regeneration stage using DI water for 30 min at -1.2 V, and thereby no discharge of ions was detected by the reading of conductivity of the flushing effluent. The mass balance on the amount of adsorbed and desorbed ions was also roughly calculated to confirm that the electrodes were completely regenerated at the end of flushing.

Successive five-cycle operation for concentrating nitrate

A 120 mL portion of real municipal wastewater effluent was fed under batch mode through the unit for 450 s under a 1.2 V electrosorption condition. The wastewater effluent was sampled from a decentralized wastewater treatment plant located in Sydney, Australia. Electrode regeneration was consequently performed circulating a fresh DI water with the same volume through the system under the same condition as electrosorption by reversing the potential. The desorbed charged species, including NO_3^-, were kept collected in the brine solution after each regeneration cycle. These electrosorption and electrode regeneration processes were successively repeated for five cycles.

Measurement of concentration of anions and their removal

The major anionic species contained in wastewater, such as NO_3^-, nitrite (NO_2^-), chloride (Cl^-), sulfate (SO_4^{2-}), and ortho-phosphate (PO_4^{3-}), were quantified using ionic chromatography (IC), (IC Thermo Fisher Scientific, Australia). All the samples were diluted properly and filtered using a 0.45 μm filter (Merck Millipore, USA) before their measurement. The calibration of IC was performed before the analyses of the samples based on external calibrations with deionized water and standard synthetic solution.

The electrosorption removal efficiency from the wastewater effluent after pilot operation was calculated using **Equation 7.1**:

$$\text{Removal efficiency (\%)} = \frac{(C_0 - C)}{C_0} \times 100 \qquad \textbf{(Equation 7.1)}$$

where C_0 and C (mg/L) are the initial and permeate concentrations of wastewater, respectively.

The electrosorption selectivity of ion *i* at time *t* can be expressed by **Equation 7.2**:

$$\text{Adsorption selectivity of i} = \frac{C_{i,t,b}}{C_{total,t,b}} \qquad \textbf{(Equation 7.2)}$$

where $C_{i,t,p}$ denotes the molar concentration of *i* and $C_{total,t,p}$ is the total molar concentration in the permeate solution at time *t*. Larger values of the adsorption selectivity imply that the ion *i* is more preferentially adsorbed from the carbon electrode over other co-existing ions.

Results and discussion

Morphology of the IX and A520E/IX layered electrodes

Since the carbon electrodes were coated with IX polymers, it is expected that the electrodes exhibit high salt adsorption capacity and effective regenerability, due to the low resistivity of the thin IX polymer layer and the elective attraction of counter-ions during electrode regeneration. Apart from this, the NO_3—selective A520E resin particles embedded in the polymer layer could lead to a more selective removal and recovery of the NO_3^- present in wastewater. The electrosorption and regeneration performances of the A520E/IX layered electrode were initially assessed, and the results were compared with the IX layered coated electrodes.

The SEM images of the surfaces of the conventional activated carbon electrode, IX and A520E/IX layered electrodes are shown in **Figure 7.1**. The nascent activated carbon electrode appeared to have a rough granular surface due to the relatively large-sized activated carbon particles (**Figure 7.1(a)**). In contrast with the virgin carbon electrode, the surface of the IX layered electrode coated with a 20 um thick anion-exchange polymer layer appeared to be smoother, confirming that the electrode surface was entirely covered with the anion-exchange polymer solution (**Figure 7.1(b)**). The NO_3—selective A520E/IX electrode, where the original carbon surface was covered by an IX layer containing A520E resin, showed a rougher surface morphology compared to the IX layer-containing electrode, due to the presence of the resin particles. It was also observed that the resin particles embedded in the IX polymer layer could not be detached from the surface easily, thus confirming that the IX solution also functioned well.

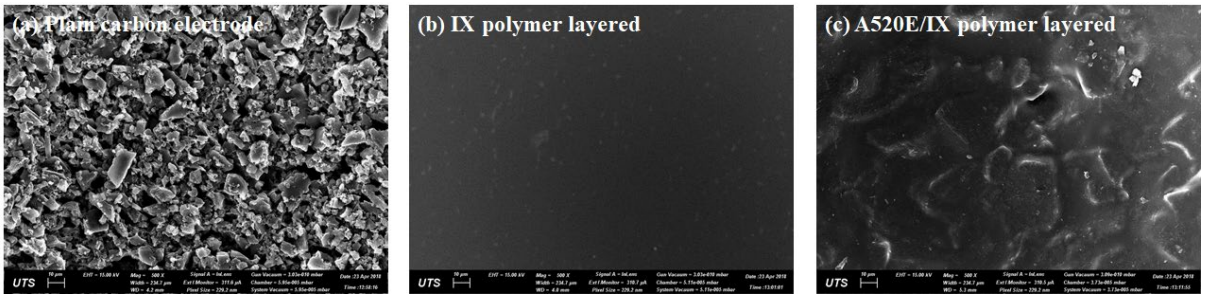

Figure 7.1. SEM images of the surface of (a) the original, (b) IX layered, and (c) A520E/IX layered carbon electrodes.

Electorosorption performance using the nitrate-selective electrode

Figure 7.2 presents the salt adsorption capacities (SAC) of NaCl and $NaNO_3$ in MCDI using the IX and A520E/IX layered carbon electrodes. The SAC of the different electrodes with a function of time t was calculated using **Equation 7.3**:

$$\text{SAC (mmol/g)} = \frac{m_t}{m} = \frac{Q \times \int_0^t (C_0 - C)dt \times M}{m} \qquad \textbf{(Equation 7.3)}$$

where m_t is the accumulative amount of adsorbed ions at time t (mmol), m is the mass of carbon on the electrode (g), Q is the flow rate of feed solution through the MCDI system (mL/min). C_0 represents the initial concentration of feed solution (mmol/L), C is the concentration of effluent at t (mmol/L), and M is the molar mass of salt (mg/mmol).

The results obtained after employing the conventional MCDI configuration using the virgin activated carbon electrodes with a separate IEM were also outlined for better understanding and comparison. The SAC values of A520E/IX layered-, IX layered-, and conventional-MCDIs were 0.252, 0.286, and 0.235 mmol/g, respectively. The higher adsorption capacity of the IX layered MCDI compared to the conventional MCDI system

was likely due to the lower resistance of the screening membrane layer yielded by the thin-coated IX layer, which functioned as an IEM directly attached on the activated carbon electrode. The low contact resistance due to the adhesion between the coating layer and the carbon surface in the IX layered MCDI could also contribute to the enhanced electrosorption and reduced energy consumption, whereas a high contact resistance was induced by the weak contact adhesion between the separate IEM and the raw carbon electrode in the conventional MCDI (Lee, Seo et al. 2011). However, the membrane layer resistance seemingly increased as the granular NO_3—selective resin particles were incorporated in the IX polymer layer, resulting in lower SAC.

The adsorption capacity for $NaNO_3$ was greater than NaCl for all the three different MCDI configurations. In general, the electrosorption capacity in solution containing single salt species can be explained by size affinity, such that the ions with smaller hydrated size possess a higher salt adsorption capacity with the electrode. Given that the hydrated radii of NO_3^- (0.335 nm) and Cl^- (0.332 nm) are similar to each other (Nightingale Jr 1959), the higher capacity for NO_3^- adsorption cannot be explained by its size-affinity to the electrical double layer (EDL). Li et al. attributed the high NO_3^- adsorption performance to its smaller hydration ratio and high electrostatic attraction toward the charged electrode surface (Li, Zhang et al. 2016). The NO_3^- was therefore likely highly attracted towards the carbon surface as a result of strong non-electrostatic attraction (Tang, Kovalsky et al. 2015).

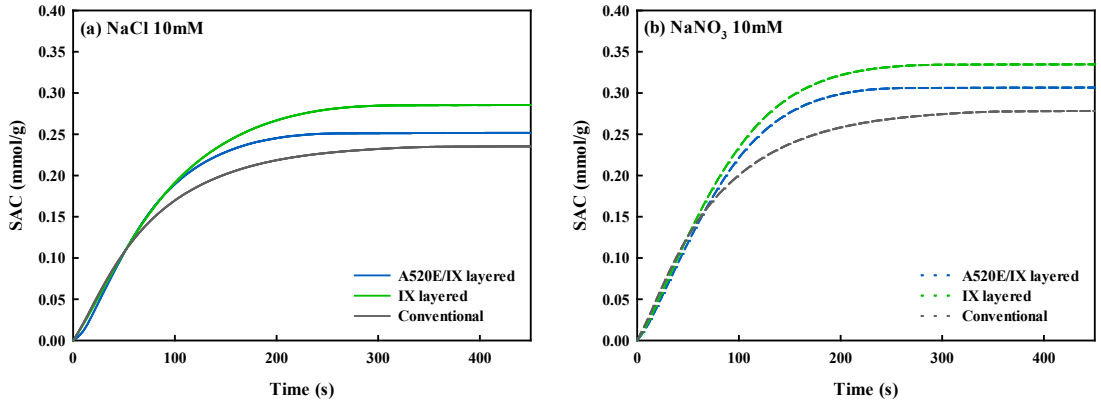

Figure 7.2. Salt adsorption capacities of A520E/IX layered-, IX layered-, and conventional- MCDIs in the removal of (a) NaCl and (b) $NaNO_3$ during experiments involving single salt species. The applied potential and feed solution flow rate during the MCDI tests were 1.2 V and 30 ml/min, respectively, under single-pass mode.

Charge efficiency can be a functional indicator of the energy efficiency of the MCDI system. Ideally, the charge efficiency is expected to be equal to unity when each electron is fully charge-balanced by the adsorption of counter-ions, and the electron transfer from an electrode to the another one is accompanied by the removal of one salt molecule from the feed water (Porada, Zhao et al. 2013).

The charge efficiency, Λ, which addresses the ratio of salt electrosorption to a such applied charge in MCDI, can be described as **Equation 7.4**:

$$\Lambda = \frac{total\ n \times F \times \int (C_0 - C) dt \times Q}{\int I dt \times A} \qquad \textbf{(Equation 7.4)}$$

where n is the number of electrons required for reduction or oxidation of one charged species, F is the Faraday's number (96485.3 C/mol), I is the current density (A/m^2), and A *is* the effective surface area of the electrode (0.01 m^2).

The energy efficiencies of the three different MCDI configurations throughout the single salt electrosorption tests were evaluated in terms of charge efficiency, as shown in **Figure 7.3**. The average charge efficiency for the conventional MCDI using the carbon electrodes with separate IEMs was 63.6%, while that of the IX layered MCDI reached up to 73.3%, which could possibly be due to the reduced interfacial resistance between the polymer layer and carbon surfaces, attributing to their strong contact adhesion (Liu, Pan et al. 2014). However, integrating the A520E resin in the anion-exchange layer increased its resistance, leading to lowered charge efficiency.

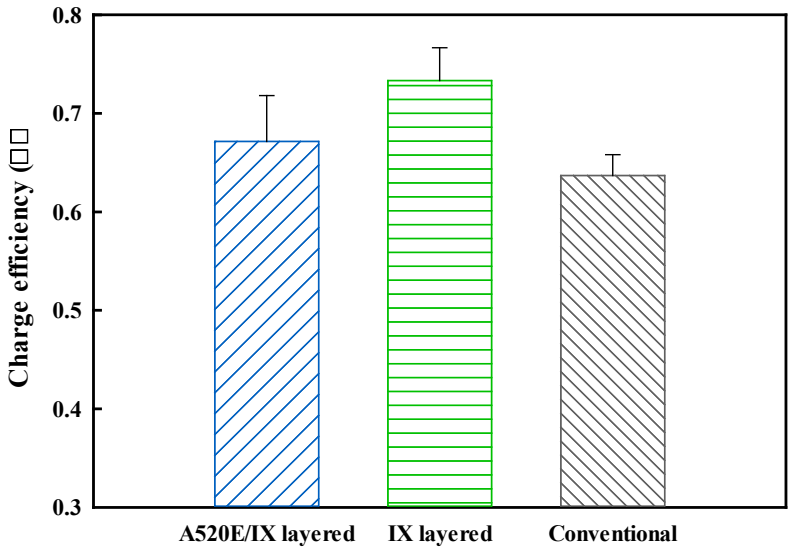

Figure 7.3. Charge efficiency among A520E/IX layered-, IX layered-, and conventional-MCDIs.

Preferential adsorption of anions in MCDI using A520E/IX layered electrodes

The phenomena of competitive removal and discharge of the selected anions in MCDI were investigated in this section using the IX layered and A520E/IX layered electrodes. As shown in **Figure 7.4(a)**, the preferential electrosorption sequence of the anions using the IX layer-coated electrodes was NO_3^- > SO_4^{2-} > Cl^-. The hydrated radii of NO_3^- and Cl^- were 0.335 and 0.332 nm, respectively (Nightingale Jr 1959), whereas their diffusion coefficients were both around 1.7 × 10-9 m^2s^{-1} (Poisson and Papaud 1983). Given the similar hydrated ionic radii and diffusion coefficients between NO_3^- and Cl^-, there has to be a reason why NO_3^- was preferably adsorbed by the IX layer-coated electrode. The better selectivity of NO_3^- was a factor of its strong hydrophobicity, thus its stronger affinity to the hydrophobic surfaces of carbon electrode allowed it to take more space in the EDL layer (Chen, Zhang et al. 2015, Hassanvand, Chen et al. 2018). Besides, the permselectivity through the IX layer also accounted for the faster electrosorption of NO_3^- (Kim, Dorji et al. 2019). NO_3^- showed a better permselectivity through the IX layer, which is highly dependent on the affinity of the anions to the membrane (Sata 2000, Luo, Abdu et al. 2018).

On the other hand, the removal preference between SO_4^{2-} and Cl^- in MCDI remains debatable in a number of previous studies. Kim et al. observed more selective adsorption of SO_4^{2-} compared to Cl^-, following the order of the general permselectivity trend through the IEM (Kim, Dorji et al. 2019). However, no apparent difference of the selectivity of SO_4^{2-} compared to the other NO_3^- and Cl^- could be found in a study of MCDI from Hassanvand et al (Hassanvand, Chen et al. 2018). Tang et al. and Yeo et al. both observed a higher selectivity in SO_4^{2-} over Cl^-, which was in accordance with our results (Yeo and Choi 2013, Tang, He et al. 2017). These studies explained that the preferential

electrosorption of SO_4^{2-} onto the electrodes was a function of the applied potential, and a higher selectivity towards SO_4^{2-} can be obtained by increasing the applied current. The gap between our results and the other studies was likely due to the different current applied on the MCDI system.

Compared to the results with the IX layered electrode, the total SAC of the A520E/IX layered electrode became lower due to the increased resistance of the polymer membrane layer, as explained in Section 7.3.1. Using the IX layered electrode, the electrosorption of all salt species appeared to have saturated at around 300 s of operation. However, it was observed that NO_3^- ions were more selectively adsorbed when the A520E resin was embedded in the IX layer coated on the carbon electrode. Furthmore, the adsorption of NO_3^- using the A520E/IX layered electrode continued to increase even longer than 450 s, whereas the adsorption of the other species (Cl^- and SO_4^{2-}) reached saturation around 300 s when the A520E/IX layered electrode was used in the MCDI tests (**Figure 7.4(b)**). Moreover, the adsorbed amount of Cl^- on the A520E/IX layered electrode decreased with the increased operation time. The mole fraction of NO_3^- with respect to the anions adsorbed on the A52E0/IX layered electrode correspondingly increased with the electrosorption time (**Figure 7.5**). Kim et al. worked on NO_3^- selective coated with BHP55 resin particles on activated carbon electrodes in conventional CDI and attributed the additional electrosorption of NO_3^- to the exchange between Cl^- on the resin coating layer and NO_3^- contained in the bulk feed solution (Kim and Choi 2012).

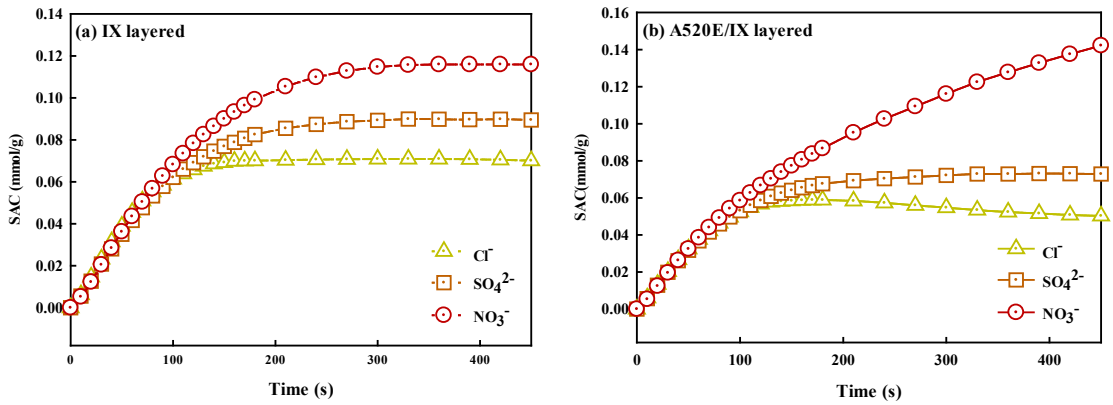

Figure 7.4. Salt adsorption capacity of the (a) IX layered- and (b) A520E/IX layered-MCDIs from a mixture of 3.3 mM of $NaNO_3$, Na_2SO_4, and NaCl, for each.

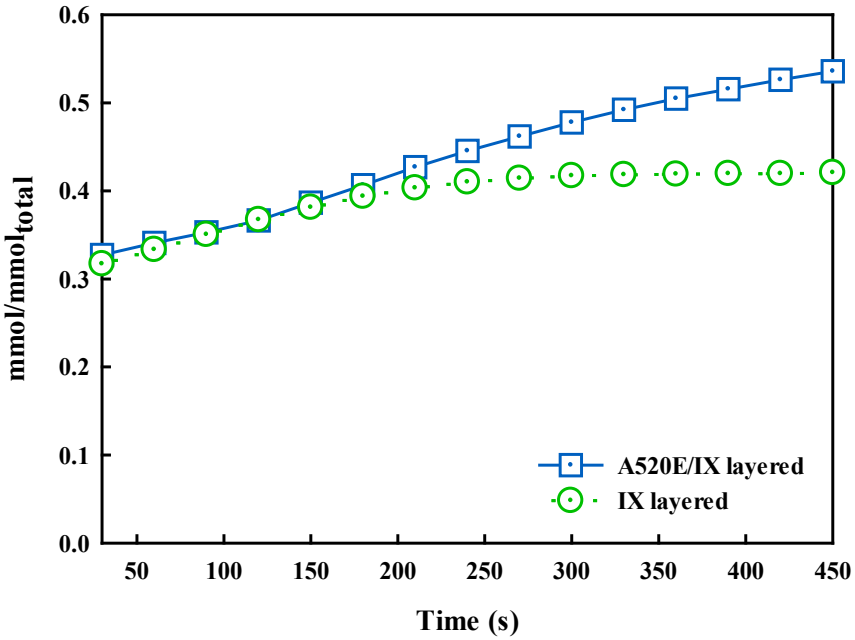

Figure 7.5. Mole fraction of adsorbed NO_3^- in the IX layered- and A520E/IX layered-MCDIs.

Preferential discharge of anions during regeneration of A520E/IX layered electrodes

The electrode regeneration step was employed under single-pass mode after the electrosorption by replacing the influent solution with DI water. The average amounts of anions captured by the IX layered electrodes throughout the experiments were 0.116, 0.090, and 0.071 mmol/g for NO_3^-, SO_4^-, and Cl^-, respectively, whereas 0.142, 0.073, and 0.050 mmol/g of NO_3^-, SO_4^-, and Cl^-, for each, was adsorbed when the A520E/IX layered electrode was used. The desorption efficiency of the anions disposed into DI water, as shown in **Figure 7.6(b) and (c)**, can be defined as the following equation.

$$\text{Desorption efficiency} = \frac{m_{d,t}}{m_a} = \frac{Q \times \int_0^t (C - C_0) dt \times M}{m_a} \qquad \textbf{(Equation 7.5)}$$

where m_a indicates the adsorbed amount of ions (mmol) on the carbon electrode, Q is the flow rate of influent (mL/min). C_0 is the initial concentration of the influent (mmol/L), C is the concentration of effluent at time t (mmol/L), and M represents the molar mass of the anion (mg/mmol).

As shown in **Figure 7.6**, NO_3^-, which was the most selectively adsorbed anionic species during electrosorption, was discharged into the DI water stream at the fastest rate for both the IX layered and A520E/IX layered electrodes. The desorption rate of the anions from both the electrodes was in the following order: $NO_3^- > SO_4^{2-} > Cl^-$ (**Figure 7.6(a) and (c)**). However, the desorption efficiencies for the anions adsorbed on the anode show different trends for the IX and A520E/IX layered electrodes. In the MCDI tests using IX layered electrodes, NO_3^- took the shortest time for being disposed among the chosen anions, while the most time was required to completely release the Cl^- (**Figure 7.6(b)**). However, the Cl^- was quickly released from the A520E/IX layered anode (**Figure 7.6(d)**). From the

A520E/IX layered electrode, Cl^- took the shortest to be disposed, whereas the longest time for was need for the desorption of NO_3^-. The retarded desorption efficiency of NO_3^- of the A520E/IX layered electrode could most likely be a result of the exchange between the NO_3^- and Cl^- during electrode regeneration (Gan, Wu et al. 2019). The reverse polarity repels NO_3^- and Cl^- ions from the EDL passing through the A520E/IX layer. However, the migrating NO_3^- would be exchanged with the Cl^- ions in the resin, thus would be temporarily intercepted at the IX layer. But at the end of the regeneration, the A520E/IX layered electrodes were found to be fully regenerated by applying reverse polarity throughout during all the experimental setups, which was consistent with the results of Kim et al (Kim and Choi 2012).

From the observations in this section of this study, the mechanism of preferential adsorption and desorption when NO_3^- selective resin is incorporated in the IX layer can be explained better. The A520E resin particles embedded in the IX polymer layer result to additional adsorption of NO_3^- on the resin coating layer, leading to enhanced selectivity of NO_3^-. However, the NO_3^- becomes the least selective species to be desorbed as the A520E resin particles trap the NO_3^- migrating from the electrode surface to the bulk effluent solution during electrode regeneration.

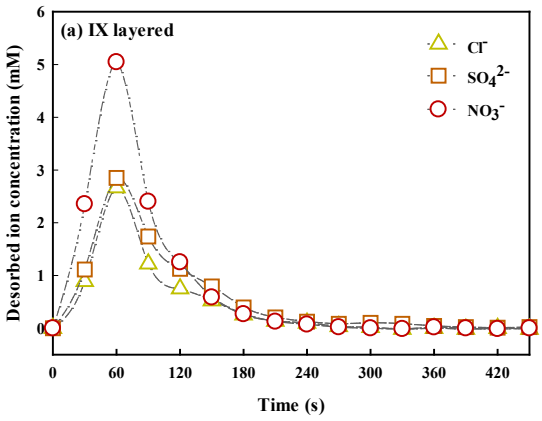

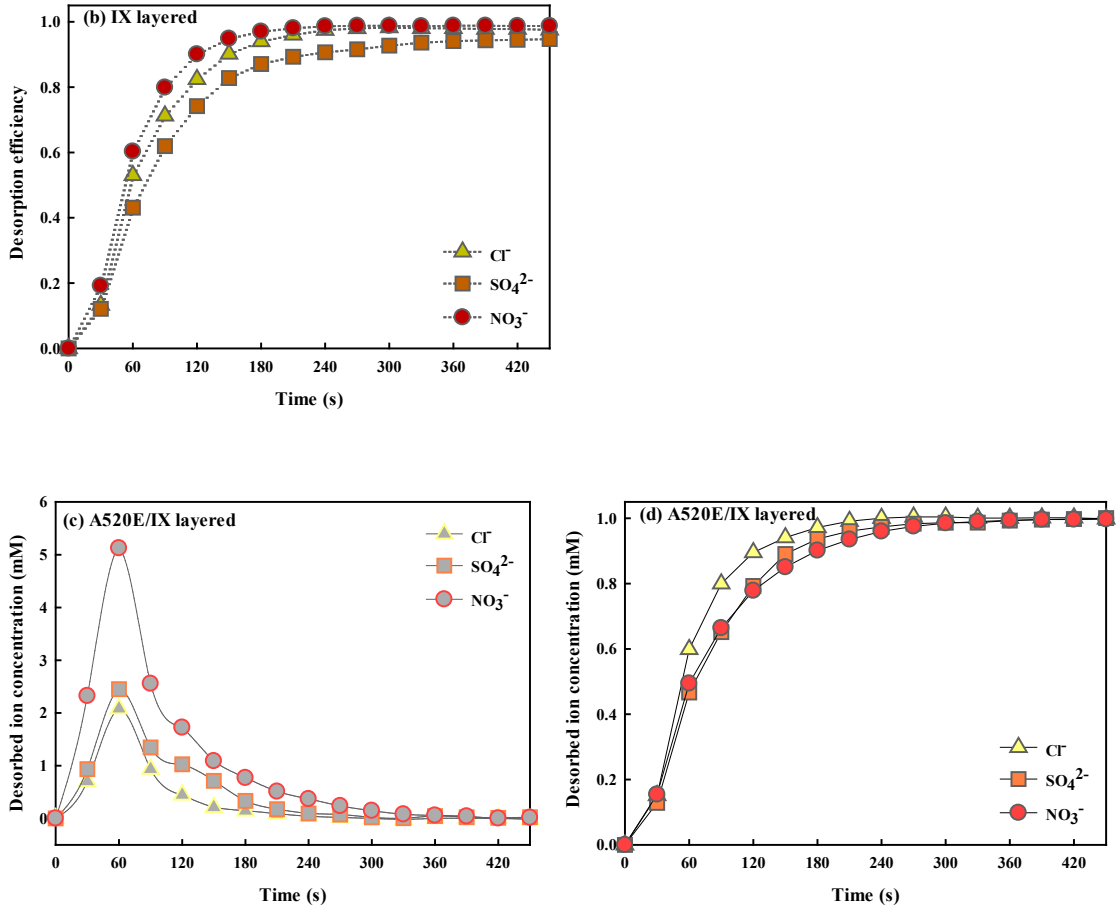

Figure 7.6. Competitive desorption among NO_3^-, Mg^{2+}, and Cl^-. The average concentrations of desorbed ions and corresponding desorption efficiency in (a and b) IX layered- and (c and d) A520E/IX layered-MCDIs.

Recovery of nitrate from real municipal wastewater effluent with A520E/IX layered electrode

In this section, the competitive removal and discharge of NO_3^- in the real municipal wastewater effluent were assessed using an IX or A520E/IX layered anode under batch mode operation. The same volume of fresh DI water was circulated through the system

under the same condition as electrosorption by reversing the potential. The desorbed ions, including NO_3^-, were collected in the brine solution after each regeneration cycle. This batch mode process was operated for five successive cycles using 120 mL of fresh wastewater effluent and 120 mL of concentrated brine solution for each test. As shown in **Figure 7.7(a)** and **Table 7.1**, the A520E/IX layered anode showed a better average removal of NO_3^-, whereas the average removal of Cl^- and SO_4^{2-} was lower than that of the IX layered one. These results imply that the A520E/IX layered electrode can selectively attract NO_3^- more, though the total removal of anionic species from the municipal wastewater was lower. As shown in **Figure 7.7(b)**, the specific selectivity in the expression of % /$\%_{total}$ using the A520E/IX layered electrode was significantly higher, whereas the SO_4^{2-} was much less preferential than the electrode coated with only the anion-exchange polymer.

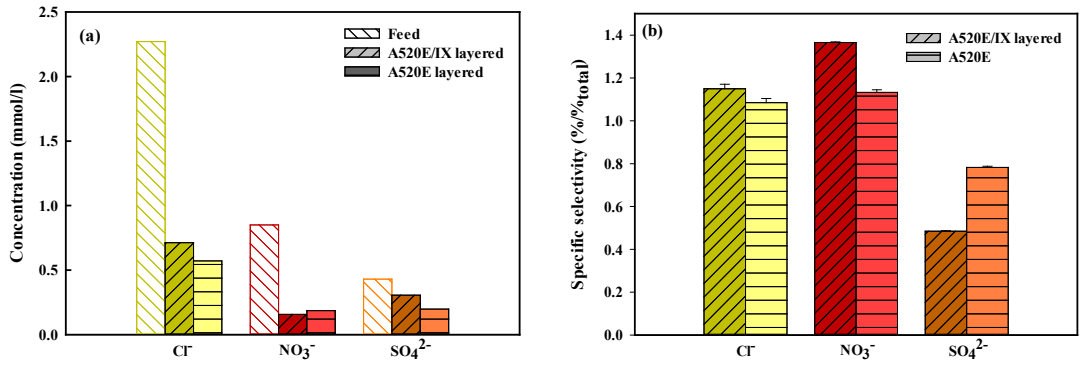

Figure 7.7. (a) Concentration of major anions in wastewater and the effluent, and the corresponding (b) specific selectivity of each ion in terms of removal %/$\%_{total}$.

Table 7.1. Ionic compositions of anions in the feed and brine solutions after five successive cycles of operation.

		Anions				
Ion		Cl^-	NO_3^-	SO_4^{2-}	TP	NO_2^-
Feed	Concentration (mM)	2.27	0.85	0.43	0.03	0.004
IX layered	Removal (%)	74.8	78.2	54.0	37.5	48.5
	1^{st} cycle brine (mM)	1.70	0.67	0.23	0.011	0.002
	3^{rd} cycle brine (mM)	4.62	1.91	0.64	0.030	0.004
	5^{th} cycle brine (mM)	7.39	3.01	0.92	0.050	0.005
	Concentration factor after 5 cycles	3.26	3.54	2.14	1.67	1.25
A520E/IX layered	Removal (%)	68.6	81.5	38.9	35.9	47.8
	1^{st} cycle brine (mM)	1.56	0.70	0.17	0.010	0.002
	3^{rd} cycle brine (mM)	4.24	1.89	0.48	0.029	0.004
	5^{th} cycle brine (mM)	6.94	3.01	0.74	0.047	0.005
	Concentration factor after 5 cycles	3.06	3.54	1.72	1.57	1.25

The discharge of the captured anions into brine solution for five cycles was directly followed by the electrosorption to enrich the NO_3^- concentration. As presented in Table 1, the NO_3^- concentration in the brine solution using IX and A520E/IX layered electrodes exhibited an almost linear increase after each cycle and reached 3.01 mM after the successive operation (3.54-fold compared to its initial concentration in the municipal wastewater feed). These results show that both the IX and A520E/IX layered electrodes can be used for successive reclamation of NO_3^- through MCDI. Given a consistent

average removal of NO_3^- (78.2 and 81.5% with IX layered and A520E/IX layered electrodes, respectively) throughout the five cycles; however, incomplete discharge of ions led to the lower brine concentration than expected. The NO_3^- concentration was correspondingly supposed to be 3.35 mM using the IX layered anode and 3.50 mM using the A520E/IX layered anode, as opposed to 3.01 mM (**Figure 7.8**). The discrepancy of the actual amount with the expected amount of NO_3^- collected was most likely a result of the constrained ion discharge efficiency when the ions in the brine solution build up a reverse ionic-strength gradient across the IEM. Previous studies attributed the retarded desorption rate during short-circuiting to the hindered ion diffusion by the concentration gradient between the phases of highly enriched brine solution and electrode surface across the IX layer (Jeon, Yeo et al. 2014, Kim, Dorji et al. 2019).

The fraction of NO_3^- in the brine solution significantly increased when the A520E/IX layered anode (**Figure 7.8**). The A520E resin in the IX layer selectively collected more NO_3^- during the electrosorption, as compared to both Cl^- and SO_4^{2-}. However, it can be noted that less of the NO_3^- adsorbed on the A520E/IX layer were less desorbed into the brine solution during electrode regeneration. Assuming the removal of NO_3^- are fixed during electrosorption and its full discharge into brine during electrode regeneration, the NO_3^- concentration in the brine after five cycles operation was supposed to be higher by using the A520E/IX layered electrode (**Figure 7.8**). The lower discharge efficiency of NO_3^- from the A520E/IX layered electrode is likely because NO_3^- was the least preferential anionic species to be desorbed, as aforementioned. These results imply that that coating the A520E/IX layer on the carbon electrode can effectively remove/recover NO_3^- through MCDI, achieving better selectively; however, its poor selectivity in discharging NO_3^- limits the enrichment of the brine solution when the high concentration

brine solution induces reverse ionic-strength gradient.

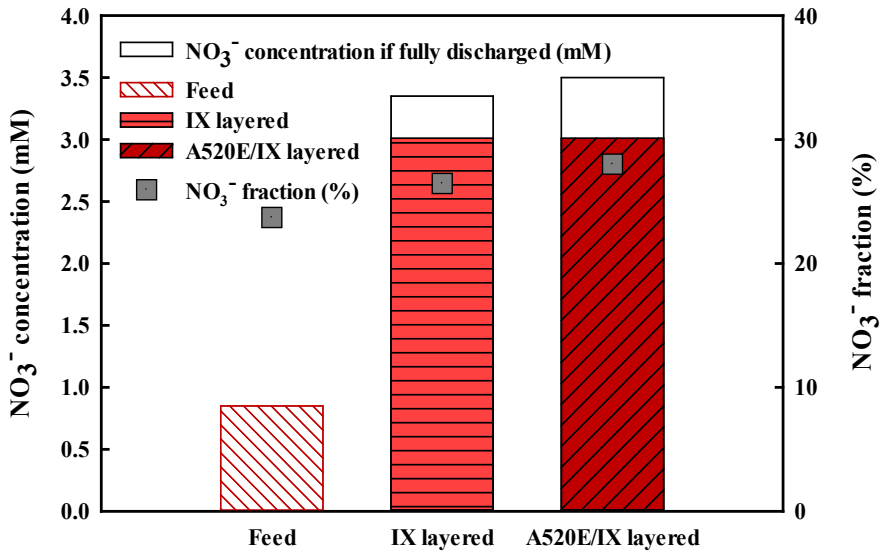

Figure 7.8. Concentration and portion of NH_4^+ in municipal wastewater feed and brine solutions after the 5th operation cycle using IX layered and A520E/IX layered electrodes.

Concluding remarks

This study systematically explored MCDI for efficient recovery of NO_3^- using a NO_3—selective IX layer coated carbon electrode. The electrosorptive performance of the coated electrodes, preferential electrosorption and desorption of three anionic species (Cl^-, SO_4^{2-}, and NO_3^-, and recovery of NO_3^- from real municipal wastewater effluent were investigated in this study.

- The coated IX polymer layer enhanced the electrosorption capacity and charge efficiency. The thin screening IX layer and tight adhesion between the carbon surface and the coated layer led to a low-contact resistance of the MCDI system. However, the electric resistivity of the electrode was increased when the granular A520E resin particles were incorporated in the IX coating layer.
- The NO_3^- was more selectively collected using the A520E/IX layered electrode. Its adsorption kept increasing even longer than 450 s, whereas the adsorption of salts reached saturation around 300 s. This was likely because the A520E resin embedded in the IX layer continued capturing NO_3^- even after the saturation of the electrode.
- The desorption rate in terms of mM/s in the effluent from both the IX layered and A520E/IX layered electrodes was in order of $NO_3^- > SO_4^{2-} > Cl^-$. However, NO_3^- took the longest time for its full desorption attributing to the exchange between the NO_3^- on the EDL and Cl^- within the IX layer during electrode regeneration.

The MCDI process with a A520E/IX layered electrode also recovered NO_3^- well from real municipal wastewater, achieving better selectivity. However, it can be noted that the least selective desorption of NO_3^-, especially when discharging into high concentration brine, was observed to limit the enrichment of the NO_3^- onto the brine.

1. aluable resources.

REFERENCES

Ansari, A. J., F. I. Hai, W. E. Price, J. E. Drewes and L. D. Nghiem (2017). "Forward osmosis as a platform for resource recovery from municipal wastewater - A critical assessment of the literature." Journal of Membrane Science **529**: 195-206.

Bae, B.-U., Y.-H. Jung, W.-W. Han and H.-S. Shin (2002). "Improved brine recycling during nitrate removal using ion exchange." Water Research **36**(13): 3330-3340.

Bahmani, P., A. Maleki, R. Rezaee, M. Khamforoush, K. Yetilmezsoy, S. Dehestani Athar and F. Gharibi (2019). "Simultaneous removal of arsenate and nitrate from aqueous solutions using micellar-enhanced ultrafiltration process." Journal of Water Process Engineering **27**: 24-31.

Batstone, D., T. Hülsen, C. Mehta and J. Keller (2015). "Platforms for energy and nutrient recovery from domestic wastewater: A review." Chemosphere **140**: 2-11.

Biesheuvel, P. M. and A. van der Wal (2010). "Membrane capacitive deionization." Journal of Membrane Science **346**(2): 256-262.

Chen, Z., H. Zhang, C. Wu, Y. Wang and W. Li (2015). "A study of electrosorption selectivity of anions by activated carbon electrodes in capacitive deionization." Desalination **369**: 46-50.

Chung, T.-S., X. Li, R. C. Ong, Q. Ge, H. Wang and G. Han (2012). "Emerging forward osmosis (FO) technologies and challenges ahead for clean water and clean energy applications." Current Opinion in Chemical Engineering **1**(3): 246-257.

Dorji, P., J. Choi, D. I. Kim, S. Phuntsho, S. Hong and H. K. Shon (2018). "Membrane capacitive deionisation as an alternative to the 2nd pass for seawater reverse osmosis desalination plant for bromide removal." Desalination **433**: 113-119.

Epsztein, R., O. Nir, O. Lahav and M. Green (2015). "Selective nitrate removal from groundwater using a hybrid nanofiltration–reverse osmosis filtration scheme." Chemical Engineering Journal **279**: 372-378.

Gan, L., Y. Wu, H. Song, S. Zhang, C. Lu, S. Yang, Z. Wang, B. Jiang, C. Wang and A. Li (2019). "Selective removal of nitrate ion using a novel activated carbon composite carbon electrode in capacitive deionization." Separation and Purification Technology **212**: 728-736.

Gao, Q., C.-Z. Wang, S. Liu, D. Hanigan, S.-T. Liu and H.-Z. Zhao (2019). "Ultrafiltration membrane microreactor (MMR) for simultaneous removal of nitrate and phosphate from water." Chemical Engineering Journal **355**: 238-246.

Hassanvand, A., G. Q. Chen, P. A. Webley and S. E. Kentish (2018). "A comparison of multicomponent electrosorption in capacitive deionization and membrane capacitive deionization." Water research **131**: 100-109.

Jeon, S.-i., J.-g. Yeo, S. Yang, J. Choi and D. K. Kim (2014). "Ion storage and energy recovery of a flow-electrode capacitive deionization process." Journal of Materials Chemistry A **2**(18): 6378-6383.

Jia, B. and L. Zou (2012). "Graphene nanosheets reduced by a multi-step process as high-performance electrode material for capacitive deionisation." Carbon **50**(6): 2315-2321.

Karamati-Niaragh, E., M. R. Alavi Moghaddam, M. M. Emamjomeh and E. Nazlabadi (2019). "Evaluation of direct and alternating current on nitrate removal using a continuous electrocoagulation process: Economical and environmental approaches through RSM." Journal of Environmental Management **230**: 245-254.

Kim, D., P. Dorji, G. Gwak, S. Phuntsho, S. Hong and H. Shon (2019). "Effect of Brine Water on Discharge of Cations in Membrane Capacitive Deionization and its Implications on Nitrogen Recovery from Wastewater." ACS Sustainable Chemistry & Engineering.

Kim, D., G. Gwak, P. Dorji, D. He, S. Phuntsho, S. Hong and H. Shon (2017). "Palladium recovery through membrane capacitive deionization (MCDI) from metal plating wastewater." ACS Sustainable Chemistry & Engineering.

Kim, D. I., P. Dorji, G. Gwak, S. Phuntsho, S. Hong and H. Shon (2019). "Reuse of municipal wastewater via membrane capacitive deionization using ion-selective polymer-coated carbon electrodes in pilot-scale." Chemical Engineering Journal **372**: 241-250.

Kim, Y.-J. and J.-H. Choi (2010). "Improvement of desalination efficiency in capacitive deionization using a carbon electrode coated with an ion-exchange polymer." Water research **44**(3): 990-996.

Kim, Y.-J. and J.-H. Choi (2012). "Selective removal of nitrate ion using a novel composite carbon electrode in capacitive deionization." Water research **46**(18): 6033-6039.

Kim, Y.-J., J.-H. Kim and J.-H. Choi (2013). "Selective removal of nitrate ions by controlling the applied current in membrane capacitive deionization (MCDI)." Journal of membrane science **429**: 52-57.

Koparal, A. S. and Ü. B. Öğütveren (2002). "Removal of nitrate from water by electroreduction and electrocoagulation." Journal of Hazardous Materials **89**(1): 83-94.

Lee, J.-Y., S.-J. Seo, S.-H. Yun and S.-H. Moon (2011). "Preparation of ion exchanger layered electrodes for advanced membrane capacitive deionization (MCDI)." Water research **45**(17): 5375-5380.

Li, H., L. Zou, L. Pan and Z. Sun (2010). "Novel Graphene-Like Electrodes for Capacitive Deionization." Environmental Science & Technology **44**(22): 8692-8697.

Li, Y., C. Zhang, Y. Jiang, T.-J. Wang and H. Wang (2016). "Effects of the hydration ratio on the electrosorption selectivity of ions during capacitive deionization." Desalination **399**: 171-177.

Liu, Y., L. Pan, X. Xu, T. Lu, Z. Sun and D. H. Chua (2014). "Enhanced desalination efficiency in modified membrane capacitive deionization by introducing ion-exchange polymers in carbon nanotubes electrodes." Electrochimica Acta **130**: 619-624.

Luo, T., S. Abdu and M. Wessling (2018). "Selectivity of ion exchange membranes: A review." Journal of membrane science **555**: 429-454.

Mendow, G., N. S. Veizaga, C. A. Querini and B. S. Sánchez (2019). "A continuous process for the catalytic reduction of water nitrate." Journal of Environmental Chemical Engineering **7**(1): 102808.

Menkouchi Sahli, M. A., S. Annouar, M. Mountadar, A. Soufiane and A. Elmidaoui (2008). "Nitrate removal of brackish underground water by chemical adsorption and by electrodialysis." Desalination **227**(1): 327-333.

Nie, C., L. Pan, Y. Liu, H. Li, T. Chen, T. Lu and Z. Sun (2012). "Electrophoretic deposition of carbon nanotubes–polyacrylic acid composite film electrode for capacitive deionization." Electrochimica Acta **66**: 106-109.

Nightingale Jr, E. (1959). "Phenomenological theory of ion solvation. Effective radii of hydrated ions." The Journal of Physical Chemistry **63**(9): 1381-1387.

Oren, Y. (2008). "Capacitive deionization (CDI) for desalination and water treatment — past, present and future (a review)." Desalination **228**(1): 10-29.

Park, J. Y. and Y. J. Yoo (2009). "Biological nitrate removal in industrial wastewater treatment: which electron donor we can choose." Applied Microbiology and Biotechnology **82**(3): 415-429.

Park, M. J., R. R. Gonzales, A. Abdel-Wahab, S. Phuntsho and H. K. Shon (2018). "Hydrophilic polyvinyl alcohol coating on hydrophobic electrospun nanofiber membrane for high performance thin film composite forward osmosis membrane." Desalination **426**: 50-59.

Park, M. J., S. Lim, R. R. Gonzales, S. Phuntsho, D. S. Han, A. Abdel-Wahab, S. Adham and H. K. Shon (2019). "Thin-film composite hollow fiber membranes incorporated with graphene oxide in polyethersulfone support layers for enhanced osmotic power density." Desalination **464**: 63-75.

Poisson, A. and A. Papaud (1983). "Diffusion coefficients of major ions in seawater." Marine Chemistry **13**(4): 265-280.

Porada, S., R. Zhao, A. Van Der Wal, V. Presser and P. Biesheuvel (2013). "Review on the science and technology of water desalination by capacitive deionization." Progress in materials science **58**(8): 1388-1442.

Porada, S., R. Zhao, A. van der Wal, V. Presser and P. M. Biesheuvel (2013). "Review on the science and technology of water desalination by capacitive deionization." Progress in Materials Science **58**(8): 1388-1442.

Sata, T. (2000). "Studies on anion exchange membranes having permselectivity for specific anions in electrodialysis—effect of hydrophilicity of anion exchange membranes on permselectivity of anions." Journal of Membrane Science **167**(1): 1-31.

Schoeman, J. J. and A. Steyn (2003). "Nitrate removal with reverse osmosis in a rural area in South Africa." Desalination **155**(1): 15-26.

Senthil Kumar, P., P. R. Yaashikaa and S. Ramalingam (2019). Efficient Removal of Nitrate and Phosphate Using Graphene Nanocomposites. A New Generation Material Graphene: Applications in Water Technology. M. Naushad. Cham, Springer International Publishing**:** 287-307.

Shannon, M. A., P. W. Bohn, M. Elimelech, J. G. Georgiadis, B. J. Marinas and A. M. Mayes (2008). "Science and technology for water purification in the coming decades." Nature **452**(7185): 301-310.

Tang, W., D. He, C. Zhang and T. D. Waite (2017). "Optimization of sulfate removal from brackish water by membrane capacitive deionization (MCDI)." Water research **121**: 302-310.

Tang, W., P. Kovalsky, D. He and T. D. Waite (2015). "Fluoride and nitrate removal from brackish groundwaters by batch-mode capacitive deionization." Water research **84**: 342-349.

Watsuntorn, W., C. Ruangchainikom, E. R. Rene, P. N. L. Lens and W. Chulalaksananukul (2019). "Comparison of sulphide and nitrate removal from synthetic wastewater by pure and mixed cultures of nitrate-reducing, sulphide-oxidizing bacteria." Bioresource Technology **272**: 40-47.

Yeo, J.-H. and J.-H. Choi (2013). "Enhancement of nitrate removal from a solution of mixed nitrate, chloride and sulfate ions using a nitrate-selective carbon electrode." Desalination **320**: 10-16.